INORGANIC CHEMISTRY FRONTIERS

RESEARCH ARTICLE

View Article Online
View Journal | View Issue

Cite this: *Inorg. Chem. Front.*, 2023, **10**, 1786

Efficient (*Z*)-selective semihydrogenation of alkynes catalyzed by air-stable imidazolyl amino molybdenum cluster sulfides†

María Gutiérrez-Blanco, [a] Eva Guillamón,[a] Vicent S. Safont, [a] Andrés G. Algarra, [b] M. Jesús Fernández-Trujillo,[b] Kathrin Junge, [c] Manuel G. Basallote, *[b] Rosa Llusar *[a] and Matthias Beller *[c]

Imidazolyl amino cuboidal $Mo_3(\mu_3\text{-}S)(\mu\text{-}S)_3$ clusters have been investigated as catalysts for the semihydrogenation of alkynes. For that purpose, three new air-stable cluster salts $[Mo_3S_4Cl_3(ImNH_2)_3]BF_4$ ([**1**]BF_4), $[Mo_3S_4Cl_3(ImNH(CH_3))_3]BF_4$ ([**2**]BF_4) and $[Mo_3S_4Cl_3(ImN(CH_3)_2)_3]BF_4$ ([**3**]BF_4) have been isolated in moderate to high yields and fully characterized. Crystal structures of complexes [**1**]PF_6 and [**2**]Cl confirm the formation of a single isomer in which the nitrogen atoms of the three imidazolyl groups of the ligands are located *trans* to the capping sulfur atom which leaves the three bridging sulfur centers on one side of the trimetallic plane while the amino groups lie on the opposite side. Kinetic studies show that the cluster bridging sulfurs react with diphenylacetylene (dpa) in a reversible equilibrium to form the corresponding dithiolene adduct. Formation of this adduct is postulated as the first step in the catalytic semihydrogenation of alkynes mediated by molybdenum sulfides. These complexes catalyze the (*Z*)-selective semihydrogenation of diphenylacetylene (dpa) under hydrogen in the absence of any additives. The catalytic activity lowers sequentially upon replacement of the hydrogen atoms of the $N\text{–}H_2$ moiety in $\mathbf{1}^+$ without reaching inhibition. Mechanistic experiments support a sulfur centered mechanism without participation of the amino groups. Different diphenylacetylene derivatives are selectively hydrogenated using complex $\mathbf{1}^+$ to their corresponding *Z*-alkenes in excellent yields. Extension of this protocol to 3,7,11,15-tetramethylhexadec-1-yn-3-ol, an essential intermediate for the production of vitamin E, affords the semihydrogenation product in very good yield.

Received 28th December 2022,
Accepted 15th February 2023

DOI: 10.1039/d2qi02755k

rsc.li/frontiers-inorganic

Introduction

The stereoselective reduction of internal alkynes to disubstituted alkenes by using hydrogen is a highly valuable reaction in the bulk and fine chemical industries.[1] In particular, (*Z*)-alkenes are found in several bioactive compounds, pharmaceuticals and agrochemicals.[2] The selective synthesis of these products has been traditionally achieved by heterogenous catalysis where the Pd-based Lindlar catalyst is still the most common choice.[3] However, for several substrates drawbacks such as isomerization and overreduction are still unsolved. Although heterogeneous catalysis is frequently preferred by industry, homogenous catalysis offers some advantages such as a more rational tuning of the catalysts as well as its potential to be used as models capable to emulate the reactivity of its solid analogues. In this regard, homogenous systems can also provide valuable mechanistic information.

Most of the reported homogeneous catalysts for the (*Z*)-stereoselective hydrogenation of alkynes to alkenes make use of alternative hydrogen donors such as boranes, silanes, alcohols, formic acid or water, while the number of systems which operate using molecular hydrogen as the reductant are surprisingly scarce.[4] Due to economic and environmental reasons, there is a growing interest to replace noble metals by non-precious ones and to optimize the atom economy using hydrogen as reductant. Most examples include mononuclear 3d transition metal complexes based on Mn,[5,6] Fe,[7] Co,[8,9] (Fig. 1) or cubane-type polynuclear Cu[10] compounds functionalized with phosphine ligands. As a very recent example, Milstein and

[a]*Departament de Química Física i Analítica, Universitat Jaume I, Av. Sos Baynat s/n, 12071 Castelló, Spain. E-mail: rosa.llusar@uji.es*
[b]*Departamento de Ciencia de los Materiales e Ingeniería Metalúrgica y Química Inorgánica, Instituto de Biomoléculas (INBIO), Facultad de Ciencias, Universidad de Cádiz, Apartado 40, Puerto Real, 11510 Cádiz, Spain*
[c]*Leibniz-Institute for Catalysis, Albert-Einstein-Street 29a, 18059 Rostock, Germany*

† Electronic supplementary information (ESI) available: NMR spectra of the synthesized compounds, UV-VIS and ESI-MS analyses. CCDC 2210047 [**1**]$PF_6{\cdot}CH_3CN$ and 2210042 [**2**]$Cl{\cdot}CH_3OH$. For ESI and crystallographic data in CIF or other electronic format see DOI: https://doi.org/10.1039/d2qi02755k

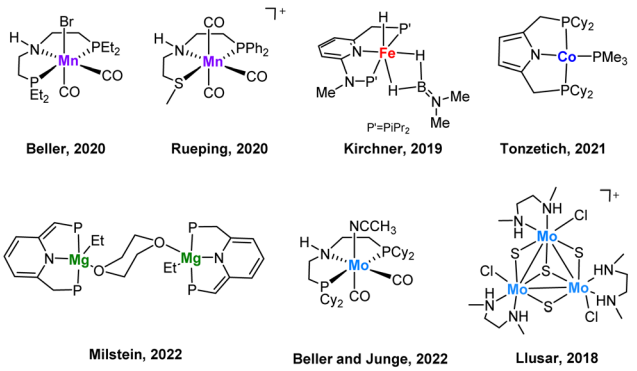

Fig. 1 Selected examples of homogeneous non-noble metal (pre)catalysts for an efficient *Z*-selective semihydrogenation of internal alkynes.

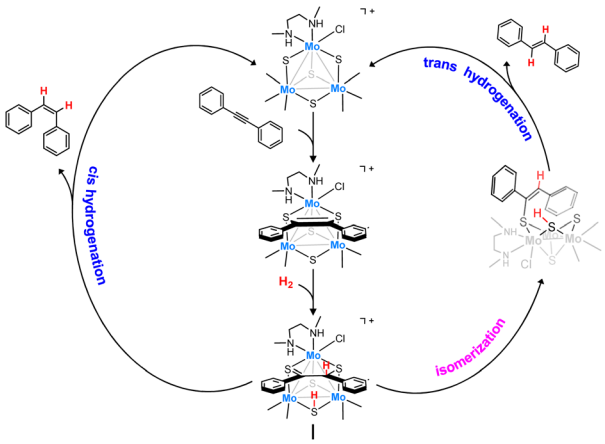

Fig. 2 Simplified catalytic cycle for the semihydrogenation of dpa in the presence of Mo_3S_4 clusters.

co-workers have evidenced the great potential of Mg pincer complexes as catalysts for the transformation of diphenylacetylene derivatives to the corresponding (*Z*)-alkenes with good to very good diastereoselectivities.[11] Previously, our groups have also shown that low-valent Mo pincer complexes and cuboidal Mo_3S_4 clusters are also efficient homogeneous catalysts for this transformation.[12,13] Notably, pincer complexes utilizing sophisticated phosphine ligands dominate this chemistry and more importantly, mechanistic investigations on these systems have revealed unique reaction pathways. Such studies combining control experiments with DFT calculations revealed that hydrogenation by PNHP and PNHS Mn and Mo pincer complexes proceeds *via* an outer sphere reaction mechanism utilizing the amino moiety in the ligand backbone for metal–ligand cooperativity.[5,6,12]

In these cases, a strong base seems to be needed to form the catalytically active species, likely an amido complex, generated by deprotonation of the amine of the ligand backbone. This amido complex presumably activates the hydrogen molecule with the corresponding formation of an $R_2(H)N$–M–H hydrido moiety where the two hydrogen atoms are transferred to the alkyne to produce the (*Z*)-alkene without any direct interaction between the substrate and the metal. On the other hand, pincer PNP complexes of Fe, Co and Mg operate under base-free conditions and H_2 activation generates catalytically active M–H hydrides, which react with the alkyne to form η^2-olefin species.[7,9] In the case of Mg, a metal–ligand cooperation mechanism (MLC) involving the aromatization/dearomatization of the pincer compound is proposed.[11]

Interestingly, trinuclear Mo_3S_4 clusters containing inexpensive diamino ligands also catalyze the semihydrogenation of diphenylacetylene (dpa) with an acceptable (*Z*)-stereoselectivity (*Z*/*E* *ca.* 6/1) in the absence of a base, albeit harsh conditions were required (12% mol catalyst, 100 bars of H_2 and 150 °C) to achieve moderate conversion (*ca.* 60%). This complex operates through an unusual cluster catalysis mechanism, depicted in Fig. 2, where only the three bridging sulfur atoms of the cluster act as the active sites for this transformation.[13]

In a first step, the alkyne molecule reacts with two of the bridging sulfides to form a dithiolene adduct. Next, hydrogen activation takes place through the third bridging sulfur atom and one of the dithiolene carbon atoms. Finally, the half-hydrogenated intermediate undergoes a reductive elimination step to produce the desired (*Z*)-alkene or to evolve into an isomerized analogue which after elimination affords the (*E*)-alkene. The relative energy barrier of these two processes, *cis*-hydrogenation *vs.* *trans* isomerization, determines the stereoselectivity of the reaction.

The low cost and low toxicity of molybdenum also makes this metal an attractive substitute to noble metals as hydrogenation catalysts although this alternative has received little attention in comparison to first row transition metals.[14,15] Motivated by our earlier results on alkyne semihydrogenation using Mo_3S_4 cluster catalysts, we decided to explore the effect of the outer bidentate ligands. Earlier studies in our group have shown that diphosphino and aminophosphino molybdenum complexes are not efficient catalysts for the direct hydrogenation of organic substrates such as nitroarenes.[16] In this work, we turned our attention to bidentate nitrogen donor ligands containing imidazolyl moieties inspired by the excellent activity in hydrogenation processes that certain noble and non-noble metal complexes, *i.e.* Ru[17,18] and Mn[19] exhibit when decorated with such imidazolyl-based ligands.

Herein, we report a novel protocol for the selective (*Z*)-semihydrogenation of a series of alkynes using a Mo_3S_4 cluster catalyst decorated with imidazolyl amino ligands. Three new cluster complexes, which differ in the nature of the amino group: $-NH_2$, $-NH(CH_3)$ and $-N(CH_3)_2$ have been prepared to investigate the influence of the Mo-amino functionality. Mechanistic experiments aimed to understand the reaction mechanism are also presented. The new $[Mo_3S_4Cl_3(ImNH_2)_3]^+$ ($\mathbf{1}^+$) complex has been applied to the catalytic semihydrogenation of several diphenylacetylene derivatives affording the (*Z*)-alkenes with excellent yields. Complex $\mathbf{1}^+$ also catalyses the semihydrogenation of an industrially relevant terminal alkyne substrate.

Experimental

General remarks

Elemental analyses were carried out on a EuroEA3000 Eurovector analyser. Electrospray mass spectra were recorded with a QuattroLC (quadrupole–hexapole–quadrupole) mass spectrometer with an orthogonal Z-spray electrospray interface (Micromass, Manchester, UK). The cone voltage was set at 20 V unless otherwise stated using CH_3CN as the mobile phase solvent. Sample solutions were infused using a syringe pump directly connected to the ESI source at a flow rate of 10 mL min^{-1} and a capillary voltage of 3.5 kV was used in the positive scan mode. Nitrogen was employed as drying and nebulizing gas. Isotope experimental patterns were compared with theoretical patterns obtained using the MassLynx 4.1 program.[20] ^1H, ^{13}C NMR and ^1H–^{13}C gradient HSQC spectra were recorded on a Bruker Avance III HD 400 MHz or 300 MHz spectrometers using CD_3CN as solvent. Gas chromatography analyses were performed on an Agilent 7820A GC system equipped with a FID and a capillary column Agilent (HP-5, 30 m × 0.32 mm × 0.25 mm). Mass determination was carried out on a GC-Mass Agilent 5977E network equipped with a mass-selective detector. Kinetic experiments on the cycloaddition of diphenylacetylene to the clusters were carried out using a Cary 50 spectrophotometer provided with a thermostatted multicell holder. All experiments were conducted at 25.0 °C under pseudo-first order conditions of alkyne excess, and the spectral changes were fitted satisfactorily in all cases to a model with a single kinetic step.

Catalyst preparation

All reactions were performed under a nitrogen atmosphere using standard Schlenk techniques. The trinuclear precursor $Mo_3S_4Cl_4(PPh_3)_3(H_2O)_2$ was prepared according to the literature procedure.[21]

Synthesis of $[Mo_3S_4Cl_3(ImNH_2)_3]BF_4$ [1]BF_4. To a green solution of the trinuclear precursor $Mo_3S_4Cl_4(PPh_3)_3(H_2O)_2$ (250 mg, 0.181 mmol) in dry CH_3CN (25 mL) was added a three-fold excess of the ligand (1-methyl-1*H*-imidazol-2-yl) methanamine (71 mg, 0.609 mmol) under inert atmosphere. The reaction occurred with an immediate colour change to brown which gradually turns into a green suspension in 1–2 hours. After stirring the reaction mixture for 4 hours at room temperature, a freshly prepared solution of HBF_4·ether (1.08 mL, 0.540 mmol) 0.5 M in CH_3CN was added and the suspension turned into a dark green solution. The solution was filtrated, taken to dryness, and redissolved in H_2O. Then, the non-soluble PPh_3 was eliminated by filtration. The resulting solution was taken to dryness and dried overnight at the vacuum pump. Finally, the product was washed with a cold mixture of hexane/toluene (1 : 1, 50 mL), boiling hexane (50 mL) and diethyl ether to afford the green solid that was characterized as $[Mo_3S_4Cl_3(ImNH_2)_3]BF_4$ (112 mg, 67% yield). Elemental analysis (%) calcd for $Mo_3S_4Cl_3C_{15}H_{27}N_9BF_4$: C 19.11, H 2.89, N 13.37; found: C 19.80, H 3.00, N 13.50; ^1H NMR (CD_3CN, 400 MHz): δ = 3.46 (br, 3H, NH, H_A), 3.81 (s, 9H, N-CH_3, H_C), 3.95 (ddd, J = 16.3, 6.0 and 1.6 Hz, 3H, CH, H_B), 4.00 (br, 3H, NH, H_A), 4.44 (ddd, J = 16.3, 7.7 and 3.4 Hz, 3H, CH, H_B), 7.48 (d, J = 1.6 Hz, 3H, CH, H_D), 8.13 (d, J = 1.6 Hz, 3H, CH, H_E); ^{13}C {^1H} NMR (CD_3CN, 101 MHz): δ = 35.28 (s, CH_2, C_C), 42.50 (s, CH_3, C_B), 125.78 (s, CH, C_D), 132.54 (s, CH, C_E), 151.54 (s, C, C_F); ESIMS (MeOH, 20 V): m/z: 856.0 [M^+].

Deuteration of $[Mo_3S_4Cl_3(ImNH_2)_3]BF_4$ [1]BF_4. A solution of 20 mg of $\mathbf{1}^+$ in 5 mL CD_3OD was kept at 50 °C overnight under continuous stirring. The solution was allowed to cool down and taken to dryness. ^1H NMR evidence the complete deuteration of the amino moiety to afford $[Mo_3S_4Cl_3(ImND_2)_3]BF_4$ [**1-d$_6$**]BF_4. ^1H NMR (CD_3CN, 300 MHz): δ 3.81 (s, 9H, N-CH_3, H_C), 3.91 (d, J = 16.3 Hz, 3H, CH, H_B), 4.41 (d, J = 16.3 Hz, 3H, CH, H_B), 7.48 (d, J = 1.6 Hz, 3H, CH, H_D), 8.13 (d, J = 1.6 Hz, 3H, CH, H_E).

Synthesis of $[Mo_3S_4Cl_3(ImNHMe)_3]BF_4$ [2]BF_4. A mixture of $Mo_3S_4Cl_4(PPh_3)_3(H_2O)_2$ (210 mg, 0.152 mmol), methyl[(1-methyl-1*H*-imidazol-2-yl)methyl]amine (65 mg, 0.494 mmol) and CH_3CN (20 mL) was stirred for 4 hours. Then, a 0.5 M solution of HBF_4·ether (1.20 mL, 0.608 mmol) in CH_3CN was added and the mixture was stirred for 30 min. The suspension was taken to dryness, redissolved in H_2O and the non-soluble PPh_3 was eliminated by filtration. The solution was concentrated under reduced pressure and the desired product was precipitated by adding THF. Finally, the resulting solid was dried at 40 °C in a vacuum oven to eliminate the water traces to give (90.8 mg, 64%) of the desired complex. Elemental analysis (%) calcd for $Mo_3S_4Cl_3C_{18}H_{33}N_9BF_4$: C 21.95, H 3.38, N 12.80; found: C 20.9, H 3.65, N 12.1; ^1H NMR (CD_3CN, 400 MHz): δ = 2.97 (d, 9H, CH_3, H_F), 3.07 (br, 3H, NH, H_A), 3.80 (s, 9H, CH_3, H_C), 3.96 (dd, J = 15.7 and 8.8 Hz, 3H, CH, H_B), 4.33 (dd, J = 15.7 and 6.6 Hz, 3H, CH, H_B), 7.45 (d, J = 1.5 Hz, 3H, CH, H_D), 7.98 (d, J = 1.6 Hz, 3H, CH, H_E); ^{13}C {^1H} NMR (CD_3CN, 101 MHz): δ = 35.22 (s, CH_2, C_C), 44.76 (s, CH_3, C_F), 51.59 (s, CH_2, C_B), 125.37 (s, CH, C_D), 132.73 (s, CH, C_E), 150.04 (s, C, C_G); ESIMS (CH_3CN, 20 V): m/z: 898.0 [M^+].

Synthesis of $[Mo_3S_4Cl_3(ImNMe_2)_3]BF_4$ [3]BF_4. A solution of $Mo_3S_4Cl_4(PPh_3)_3(H_2O)_2$ (100 mg, 0.073 mmol) was reacted with dimethyl[(1-methyl-1*H*-imidazol-2-yl)methyl]amine (35 mg, 0.240 mmol) in CH_3CN (15 mL). The colour of the solution turned out to brown and stirring continued for 5 hours. Next, a 0.5 M solution of HBF_4·ether complex (0.58 mL, 0.2916 mmol) in CH_3CN was added dropwise and the solution turned green. After 30 minutes, the solution was filtrated, taken to dryness, and redissolved in MeOH. The desired product was precipitated by adding diethyl ether (50 mL). Finally, the green solid was separated by filtration and washed with a cold mixture of hexane/toluene (1 : 1, 50 mL), boiling hexane (50 mL) and diethyl ether to yield an air-stable product characterized as $[Mo_3S_4Cl_3(ImNMe_2)_3]BF_4$ (70.3 mg, 94%). Elemental analysis (%) calcd for $Mo_3S_4Cl_3C_{15}H_{27}N_9BF_4$: C 24.56, H 3.83, N 12.28; found: C 25.38, H 3.78, N 11.90; ^1H NMR (CD_3CN, 400 MHz): δ = 2.96 (s, 18H, CH_3, H_A), 3.91 (s, 9H, CH_3, H_C), 4.61 (s, 6H, CH_2, H_B), 7.53 (d, J = 2.0 Hz, 3H, CH, H_D), 7.56 (d, J = 2.0 Hz, 3H, CH, H_E); ^{13}C {^1H} NMR (CD_3CN, 101 MHz): δ = 36.59 (s, CH_3, C_C), 44.85 (s, CH_3, C_A),

49.28 (s, CH_2, C_B), 122.45 (s, CH, C_D), 127.02 (s, CH, C_E), 136.33 (s, C, C_F); ESIMS (CH_3CN, 20 V): *m/z*: 940.0 [M^+].

X-ray data collection and structure refinement

Suitable crystals for X-ray studies of complex $\mathbf{1}^+$ were obtained by slow evaporation of a sample of [**1**]BF_4 in CH_3CN the presence of an excess of NH_4PF_6. Crystals of $\mathbf{2}^+$ were grown by slow evaporation of a sample solution of $\mathbf{2}^+$ in CH_3OH acidified with HCl. Diffraction data collection was performed at 200 K on an Agilent Supernova diffractometer equipped with an Atlas CCD detector using $Cu_{K\alpha}$ radiation (λ = 1.54184 Å). No instrument or crystal instabilities were observed during data collection. Absorption corrections based on the multiscan method were applied.[22,23] The structure was solved by direct methods and refined by the full-matrix methods based on F^2 with the program SHELXL-13 using the Olex2 software package.[24,25] Graphics were performed with the Diamond visual crystal structure information system software.[26]

Crystal data for [1]PF_6·CH_3CN. $C_{17}H_{30}Cl_3F_6Mo_3N_{10}PS_4$, M = 1041.89, triclinic; space group $P\bar{1}$, a = 10.2357(3), b = 12.7929 (3), c = 13.9167(4) Å; α = 68.076(3)°, β = 84.513(2)°, γ = 81.883 (2)°; V = 1671.76(8) Å^3; T = 200.00(14); Z = 2; μ(MoK_α) = 14.717 mm^{-1}; reflections collected/unique = 34 375/6824 (R_{int} = 0.0664). The final refinement converged with R_1 = 0.0400 and wR_2 = 0.0881 for all reflections, GOF = 1.0340 a $d_{max./min}$ residual electron density 0.96/−0.84 e Å^{-3}.

Crystal data for [2]Cl·CH_3OH. $C_{19}H_{37}Cl_4Mo_3N_9OS_4$, M = 965.43, triclinic; space group $P\bar{1}$, a = 9.67045(18), b = 12.8501 (2), c = 13.6166(3) Å; α = 79.6676(15)°, β = 86.3570(15)°, γ = 88.6075(14)°; V = 1661.14 Å^3; T = 200.00(14); Z = 2; μ(CuK_α) = 1.710 mm^{-1}; reflections collected/unique = 30 528/6409 (R_{int} = 0.00272). The final refinement converged with R_1 = 0.0302 and wR_2 = 0.0684.

The structures of the complex salts [**1**]PF_6·CH_3CN and [**2**]Cl·CH_3OH were refined in the triclinic $P\bar{1}$ space group. The non-hydrogen atoms of the clusters and the counterions were refined anisotropically, whereas the positions of all hydrogen atoms in the ligands were generated geometrically, assigned isotropic thermal parameters, and allowed to ride on their respective parent carbon atoms. In both cases the solvent molecules in the crystal were refined anisotropically and their hydrogen atoms were included at their idealized positions.

CCDC 2210047 and 2210042† contains the supplementary crystallographic data for this paper.

Catalytic activity tests

General procedure for hydrogenation experiments. A 4 mL glass vial containing a stirring bar was sequentially charged with the corresponding molybdenum catalyst, alkyne (0.1 mmol), *n*-hexadecane (15 μL; added as an internal standard) and 2 mL of dry CH_3CN. Afterwards, the reaction vial was capped with a screw cap containing a septum with a needle and set in the alloy plate, which was then placed into a 300 mL autoclave. The sealed autoclave was purged three times with 30 bar of hydrogen before the desired pressure was set. Then, it was placed into an aluminium block which was preheated with the desired temperature. After 18 h, the autoclave was cooled to room temperature and the hydrogen was released. Ethyl acetate (2 mL) was then added, and a sample was analyzed by GC. To determine the isolated yield of alkenes, the reaction was scaled up by the factor of three, and no internal standard was added. After completion of the reaction, the mixture was taken to dryness, solved in pentane, and filtered through silica. The solvent was removed *via* rotary evaporation and dried under vacuum.

Results and discussion

Synthesis and characterization

Three new trinuclear cluster salts of formula [$Mo_3S_4Cl_3(ImNH_2)_3$]BF_4 ([**1**]BF_4), [$Mo_3S_4Cl_3(ImNH(CH_3))_3$]$BF_4$ ([**2**]BF_4) and [$Mo_3S_4Cl_3(ImN(CH_3)_2)_3$]$BF_4$ ([**3**]BF_4) have been prepared by extending the procedure developed in our group and represented in Scheme 1.[27] In this method the outer ligands of the $Mo_3S_4Cl_4(PPh_3)_3(H_2O)_2$ precursor are partially replaced by imidazolylamino ligands. Acidification of the reaction media avoids formation of hydroxo species which result from the partial replacement of the outer chlorine ligands. As found for the aminophosphine M_3S_4 (Mo or W) derivatives, only one among all possible isomers is formed in moderate to high yields, 67% for [**1**]BF_4, 64% for [**2**]BF_4 and 94% for [**3**]BF_4.[28] All clusters salts were fully characterized by NMR, elemental analysis, and mass spectrometry.

The crystal structures of [**1**]PF_6 and [**2**]Cl have been determined by single crystal X-ray diffraction and they share structural features. Fig. 3 and 4 show ORTEP representations of the $\mathbf{1}^+$ and $\mathbf{2}^+$ cations together with relevant bond distances. Both cations contain an incomplete Mo_3S_4 cubane-type structure in which the molybdenum and sulfur atoms occupy adjacent vertices with a missing metal atom. In general, the metal–metal and metal–sulfur bond distances follow the same tendencies observed for other trinuclear Mo_3S_4 species.[27,29] The three outer positions on each metal center are occupied by one chlorine atom and two nitrogen atoms from the imidazolyl amino ligand.

As previously mentioned, only one isomer is formed, wherein all three nitrogen atoms from the imidazolyl group are located *trans* to the capping sulfur while the ones from the amino group are placed *trans* to the bridging sulfur. Therefore, the capping sulfur, the chlorine atoms, and the amino groups of the ligand lie on the same side of the trimetallic plane.

The short Cl···H(–N) distances in $\mathbf{1}^+$ (2.458 to 2.802 Å) and $\mathbf{2}^+$ (2.359 to 2.951 Å) between the chlorine atom and the hydro-

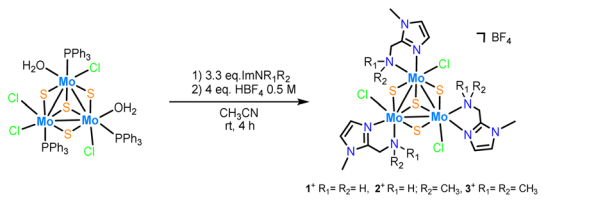

Scheme 1 Synthesis of Mo_3S_4 cluster complexes decorated with imidazolylamino ligands.

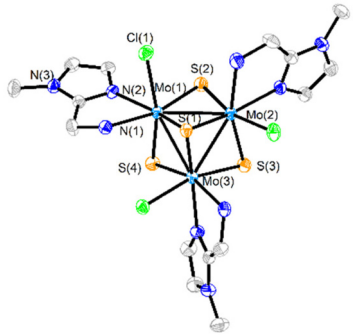

Fig. 3 ORTEP representation (50% probability ellipsoids) of the cationic cluster $[Mo_3S_4Cl_3(ImNH_2)_3]$ + ($\mathbf{1}^+$). Hydrogen atoms have been omitted for clarity. Standard deviations of average distances are given in brackets. Average bond distances: Mo–Mo = 2.7378 [7], Mo-(μ3-S) = 2.328 [2], Mo-$(\mu\text{-S})_{trans\text{-Cl}}$ = 2.28 [1], Mo-$(\mu\text{-S})_{trans\text{-NH}_2}$ = 2.29 [1] Å.

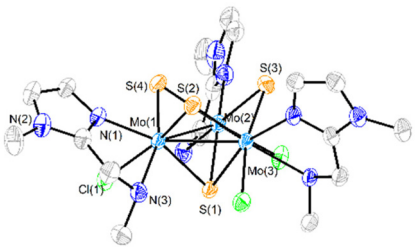

Fig. 4 ORTEP representation (50% probability ellipsoids) of the cationic cluster $[Mo_3S_4Cl_3(ImNHCH_3)_3]^+$ ($\mathbf{2}^+$). Standard deviations of average distances are given in brackets. Hydrogen atoms have been omitted for clarity. Average bond distances: Mo–Mo = 2.759 [3], Mo-$(\mu_3\text{-S})$ = 2.338 [4], Mo-$(\mu\text{-S})_{trans\text{-Cl}}$ = 2.288 [6], Mo-$(\mu\text{-S})_{trans\text{-NHMe}}$ = 2.289[6] Å.

gen atom of the amino groups of the adjacent metal center evidence the presence of hydrogen bonding interactions. Moreover, in the case of complex $\mathbf{1}^+$ the above-mentioned values are comparable to the Cl···H(–N) distances of the chlorine atom and the amino group on the same metal center, with values ranging from 2.747 to 2.938 Å.

The solid-state structures of both cations, $\mathbf{1}^+$ and $\mathbf{2}^+$, are preserved in solution as evidenced by ^{13}C NMR and ^{1}H NMR spectroscopy. All attempts to obtain single crystals of $\mathbf{3}^+$ were unfruitful but the product was fully characterized by spectrometric and spectroscopic techniques. The C_3 symmetry of the three complexes has been confirmed in solution (Fig. SI1–SI6†). The ^{13}C NMR spectra show five characteristic singlets, common for all three compounds, four signals of the imidazole ring and one to the methylene linker group. Nevertheless, the ^{1}H NMR spectrum of $\mathbf{3}^+$ reveals a slightly different solution behaviour compared to that of the other two clusters. In clusters $\mathbf{1}^+$ and $\mathbf{2}^+$, the signals for the methylene hydrogen atoms are clearly diastereotopic with resolved multiplets showing both the germinal coupling and the coupling to the amino hydrogen/s in agreement with their crystal structures. In contrast, this multiplet signal appears as a singlet in compound $\mathbf{3}^+$, which suggests the existence of a weak Mo-NMe_2 bond that allows for rapid dissociation–coordination and results in a time-averaged signal for the two methylene protons.

Reactivity *versus* alkynes and reaction kinetics

As mentioned in the Introduction, formation of dithiolene adducts upon interaction of alkynes with the bridging sulfur atoms of the cuboidal Mo_3S_4 unit is the first step of the mechanism for the semihydrogenation of alkynes catalyzed by these cluster complexes.[13] It is well stablished that the [3 + 2] cycloaddition reaction between the alkynes and these clusters, depends on the alkyne substituents as well as on the nature of the cluster ligands.[30,31] Formation of very stable Mo_3S_4 dithiolene adducts is detrimental for the catalytic semihydrogenation of alkynes. For example, the $[Mo_3S_4Cl_3(dmen)_3]^+$ (dmen = *N*,*N*′-dimethylethylenediamine) cluster reacts with dimethyl acetylcarboxylate (dmad) to form a stable adduct and as a consequence it is not an active catalyst for alkyne semihydrogenation. On the other hand, the $[Mo_3S_4Cl_3(dmen)_3]^+$ cluster does not react appreciably with diphenylacetylene (dpa), and thus it catalyzes its semihydrogenation although under harsh conditions. In our case, cluster complexes [**1**]BF_4, [**2**]BF_4 and [**3**]BF_4 react with dpa to form the corresponding dithiolene adduct as evidenced by the appearance of a band in the UV-VIS spectra around 900 nm, characteristic of the formation of the [3 + 2] cycloaddition product (Fig. SI7†).[32] Adduct formation is also evidenced by ^{1}H NMR spectroscopy where new signals appear due to the loss of symmetry upon adduct formation (Fig. SI8†).[21] However, these new signals coexist with those of $\mathbf{1}^+$, $\mathbf{2}^+$ and $\mathbf{3}^+$ which indicates that formation of the addition dithiolene products occur under conditions of reversible equilibrium. This assumption is further confirmed by the electrospray ionization mass spectrometry (ESI-MS) of the reaction mixture (Fig. SI9†). The ESI-MS spectrum of $\mathbf{1}^+$ in CH_3CN shows a prominent peak centered at m/z = 856 associated to the $\mathbf{1}^+$ cation according to its m/z value and calculated isotopic pattern. Upon reaction with an excess of dpa (20 eq., room temperature, CH_3CN), the peak at m/z = 856 remains and a new peak of similar intensity emerges at m/z = 1034 identified as the [**1** + dpa]$^+$ cycloaddition product. Incidentally, no evidence exists regarding the addition of a second dithiolene molecule. A similar situation is observed when monitoring the reaction between [**2**]BF_4 and [**3**]BF_4 with dpa in CH_3CN. That is, the cluster cations coexist with the cycloaddition dithiolene adduct even in the presence of a 20 molar excess of dpa.

To obtain additional information on the process, the kinetics of reaction of [**1**]BF_4, [**2**]BF_4 and [**3**]BF_4 with dpa were studied in acetonitrile solutions at 25 °C. The reaction was found to occur in a timescale suitable for monitoring the process with a conventional UV-VIS spectrophotometer. The spectral changes observed under pseudo-first order conditions of dpa excess (Fig. SI7†) clearly show the formation of the cycloaddition product with the previously commented band at 900 nm. These changes can be satisfactorily fitted using a kinetic model with a single kinetic step, and the values derived for the observed rate constant (k_{obs}) show a linear dependence with the alkyne concentration that was fitted

using eqn (1) (Fig. 5). The values so derived for the slope and the intercept are listed in Table 1.

$$k_{obs} = k_0 + k_1[\text{dpa}] \quad (1)$$

In agreement with the NMR and ESI-MS results, the existence of a non-zero intercept in Fig. 5 suggests the possibility that the reaction occurs under conditions of reversible equilibrium, which is confirmed by an increase of the spectral change magnitude with the dpa concentration, so that k_1 corresponds to the formation of the cycloaddition product, and k_0 to the reverse process. While the rate of formation (k_1) decreases gradually with the number of the amino methyl groups of the ligand, the rate of the reverse reaction (k_0) shows smaller changes. Therefore, the equilibrium constant decreases upon methylation of the amino groups of the ligand. These results differ from those previously reported for the related diamino cluster, for which we were unable to observe formation of significant amounts of the cycloaddition product.[13]

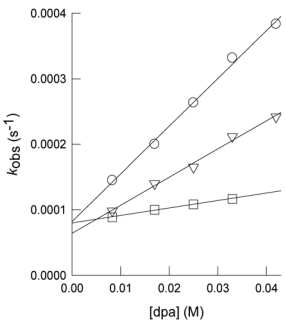

Fig. 5 Plot of the dependence with the dpa concentration of the observed rate constants for the reaction of clusters [**1**]BF_4 (circles), [**2**]BF_4 (triangles), and [**3**]BF_4 (squares), with an excess of dpa in CH_3CN solutions at 25 °C.

Table 1 Kinetic data for the reaction of [**1**]BF_4, [**2**]BF_4 and[**2**]BF_4 with an excess of dpa[a]

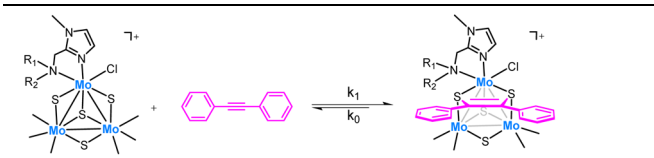

1$^+$ R_1= R_2= H, **2**$^+$ R_1= H; R_2= CH_3, **3**$^+$ R_1= R_2= CH_3

Entry	Cluster	k_1 (M^{-1} s^{-1})	k_0 (s^{-1})	K_e (M^{-1})
1	**1**$^+$	$7.3(3) \times 10^{-3}$	$8.2(7) \times 10^{-5}$	89(8)
2	**2**$^+$	$4.3(2) \times 10^{-3}$	$6.4(6) \times 10^{-5}$	67(7)
3	**3**$^+$	$1.14(4) \times 10^{-3}$	$8.0(1) \times 10^{-5}$	14.0(5)

[a] Reaction conditions: 25 °C in CH_3CN, pseudo-first order excess of dpa (0.008–0.042 M).

Catalytic performance and mechanistic insights

Evaluation of the catalytic activity of [**1**]BF_4, [**2**]BF_4 and [**3**]BF_4 was performed on the semihydrogenation of diphenylacetylene as model reaction. Reaction conditions for the [**1**]BF_4 cluster salt catalyst were optimized by varying the temperature and H_2 pressure (Table SI1†). Full conversion and quantitative yield towards the formation of the (*Z*)-isomer was achieved under much milder conditions (70 °C and 20 bar) compared to previously known related molybdenum catalysts. For example, a conversion of 21% (18% of the (*Z*)-isomer and 3% of the (*E*)-isomer) was obtained using the diamino $[Mo_3S_4Cl_3(dmen)_3]^+$ cluster catalyst (18 h at 150 °C, 100 bar H_2 pressure and 5 mol% of the catalyst) in acetonitrile.[13] Further attempts to lower the pressure and/or temperature led to a dramatic decrease of the catalytic activity. Incidentally, our optimized conditions are the typical conditions employed for the hydrogenation of nitroarenes mediated by the diamino $[Mo_3S_4Cl_3(dmen)_3]^+$ catalyst.[16] Then, the solvent influence was investigated. Similar activities are found for CH_3CN and CH_3OH (Table SI2†) while THF reduced the dpa conversion to 90%. No reaction is observed in 2-fluoroethanol or hexafluoroisopropanol. Hence at this point, we decided to continue the study in CH_3CN.

Cluster evolution during the catalytic semihydrogenation of dpa using [**1**]BF_4 was monitored from batch experiments at different reaction times (Fig. SI10†). The molecular peak due to **1**$^+$ (m/z = 856) coexists with the [**1** + dpa]$^+$ (m/z = 1034) cycloaddition product. As expected, the intensity of the [**1** + dpa]$^+$ peak decreases with time. At the end of our catalytic protocol, the only peak registered, that of **1**$^+$, remains intact; therefore, catalysis occurs without degradation of **1**$^+$ which is indicative of a cluster catalysis process.

Next, we investigated the influence of the structure of the ligand on the catalytic activity for the semihydrogenation of diphenylacetylene at 70 °C and 20 bars of H_2 (Table 2, entries 2–4). Substitution of one hydrogen of the N–H moiety in **1**$^+$, leads to a significant decrease in the catalytic activity (Table 2, entry 2). The total alkylation of the N–H moiety (Table 2, entries 3 and 4) with methyl substituents does not inhibit the catalytic conversion but drastically lowers the yield. The activity of **3**$^+$ is comparable with that of the diamino $[Mo_3S_4Cl_3(dmen)_3]BF_4$ catalysts (Table 2, entry 5).[13]

An extra evidence of the passive role of the N–H moiety is that no deuterated (*Z*)-stilbene (Fig. SI11†) was formed by using the **1-d$_6$**$^+$ cluster catalyst (Fig. SI12†) deuterated at the amino positions (Table 2, entry 6). These experiments rule out the involvement of the N–H moiety of the ligand backbone in the reaction. In contrast, there are strong evidences on metal–ligand cooperativity when low-valent molybdenum PN^HP pincer complexes are employed as catalysts for this transformation which give support in this last case to an outer sphere reaction mechanism.[12]

Then, mechanistic evidence for a sulfur-based reaction mechanism were investigated. For that purpose, CuCl was added to the catalytic reaction mixture in order to block the three bridging sulfur atoms of the cluster. According to ESI-MS

Table 2 Evaluation of conditions for diphenylacetylene (dpa) hydrogenation[a]

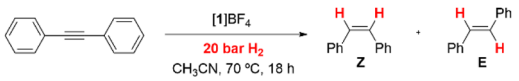

Entry	Deviation	Conversion[b] [%]	Yield[b] [%] Z	E
1	None	>99	>99	—
2	[**2**]BF_4	40	40	—
3	[**3**]BF_4	7	7	—
4	[**3**]BF_4 [c]	23	23	—
5	$[Mo_3S_4Cl_3(dmen)_3]BF_4$ [d]	13	10	3
6	$[Mo_3S_4Cl_3(ImND_2)_3]BF_4$ [e]	>99	>99	—
7	Addition of CuCl	0	—	—
8	Addition of Et_3N (1 equiv.)	30	29	—
9	Addition of Et_3N (2 equiv.)	7	7	—
10	Addition of Et_3N (3 equiv.)	7	7	—

[a] Standard conditions: diphenylacetylene (0.1 mmol), H_2 pressure (20 bar), 70 °C, catalyst (5 mol%), CH_3CN, 18 h. [b] Determined by GC analysis using *n*-hexadecane as an internal standard. [c] Catalyst (12 mol%). [d] Catalyst (12 mol%) H_2 pressure (50 bar), 150 °C. [e] Stoichiometric reaction, 0.01 mmol diphenylacetylene, 0.01 mmol cluster [**1-d$_6$**]BF_4, CD_3CN.

formation of the heterometallic $[Mo_3(CuCl)S_4Cl_3(ImNH_2)_3]^+$ (*m*/*z* = 956) and $[Mo_3(Cu(dpa))S_4Cl_3(ImNH_2)_3]^+$ (*m*/*z* = 1099) cluster cations took place on the basis of their *m*/*z* ratios and isotopic pattern (Fig. SI13†). Under these conditions, the catalytic process is inhibited (Table 2, entry 7) as previously observed for the semihydrogenation of alkynes and hydrogenation of diazobenzene mediated by the diamino $[Mo_3S_4Cl_3(dmen)_3]^+$ catalysts, which was also attributed to the formation of Mo_3S_4Cu species.[13,33]

In the case of the catalytic diazobenzene hydrogenation, hydrogen activation occurs at the bridging sulfur atoms and results in the formation of a dithiol $[Mo_3S_2(SH)_2Cl_3(dmen)_3]^+$ adduct from which hydrogen is transferred to form first diphenylhydrazyne and next aniline through two interconnected cycles sharing a common reaction step which involves the above Mo_3S_4 dithiol adduct.[33] Due to the acidic character of this proton S–H groups, addition of a base such as Et_3N inhibits the hydrogenation process by providing an additional reaction pathway which capture these dithiol H atoms. In our case, the same tendency has been observed and addition of Et_3N amine inhibits catalysis (Table 2, entries 8–10) suggesting a mechanism for hydrogen activation in which acidic protons are being generated.

The above control experiments indicate a sulfur-centered cluster catalysis mechanism without metal–ligand cooperativity. However, details on H_2 activation by the bridging sulfur atoms of the cluster and their subsequent transfer to the alkyne molecule to selectively afford the (*Z*)-alkene remain unclear.

Substrate scope

Having in hand the optimal conditions for dpa semihydrogenation mediated by [**1**]BF_4, dpa derivatives featuring different substituents were tested to analyze the tolerance of the system (Table 3).

Compounds containing a methyl group in the *para* (**2c**) and *meta* (**2b**) positions were successfully reduced with excellent selectivity. However, in the case of the *ortho* derivative (**2b**) there was a drop of the conversion likely due to steric hindrance.[12,34] Alkynes bearing halides as fluorine, chlorine, bromine or trifluoromethyl groups are smoothly transformed to the respective (*Z*)-alkenes. Remarkably, no dehalogenation products have been detected for any of the halogenated dpa derivatives. Also, substrates containing both trifluoromethyl and methoxy groups (**2i**) afforded good yields and stereoselectivity. Additionally, thioethers (**2j**) or ester groups (**2k**) on the alkynes are well tolerated.

Taking into consideration that [**1**]BF_4 is an efficient catalyst for the semihydrogenation of internal alkynes, we decided to extend our study to terminal alkynes. The industrially relevant substrate chosen was 3,7,11,15-tetramethylhexadec-1-yn-3-ol, represented in Fig. 6, which is an essential intermediate for the production of vitamin E.[35] Application of the optimized catalytic protocol developed for dpa semihydrogenation results in no conversion of the terminal alkyne substrate.

Table 3 (*Z*)-selective semihydrogenation of alkynes catalyzed by [**1**]BF_4[a]

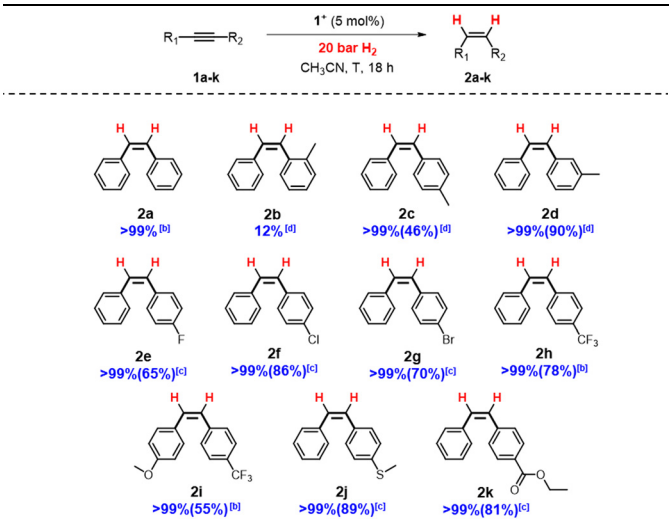

[a] Reaction conditions: 0.1 mmol alkyne, 5 mol% catalyst, 20 bar H_2, CH_3CN (2 mL), 18 h. Yield determined by GC analysis using *n*-hexadecane as an internal standard (average of two runs). Isolated yields are given in brackets. [b] *T* = 60 °C. [c] *T* = 70 °C. [d] *T* = 80 °C.

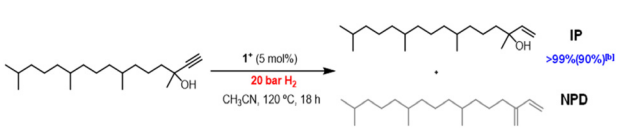

Fig. 6 Semihydrogenation of DIP. Reaction conditions: 0.1 mmol alkyne, 5 mol% catalyst, 20 bar H_2, 120 °C, CH_3CN (2 mL), 18 h. Conversions and yields determined by GC analysis using *n*-hexadecane as an internal standard.

Temperature and pressure were then optimized (Table SI3†) and quantitative conversions were achieved at 120 °C and 20 bar H_2. In terms of chemoselectivity, the major product is the desired isophytol (IP). Notably, no over hydrogenation product was observed during the reaction and the only detected side product corresponds to the dehydration species, neophytadiene (NPD). Then, the influence of the reaction time was investigated to hamper this side-reaction (see Fig. SI32†). While the reaction time can be reduced from 18 h to 8 h maintaining conversion and yield, this has no effect on the final NPD concentration. Unfortunately, all attempts to avoid this side reaction were unfruitful. To the best of our knowledge, it is the first time that a homogenous molybdenum cluster performs this reaction. Further experiments are under investigation to achieve softer conditions.

Conclusions

In summary, we have synthesized and characterized three new Mo_3S_4 complexes featuring imidazolyl amino ligands with different degrees of methylation in the amino moiety. The bridging sulfur atoms of these $Mo_3(\mu_3\text{-}S)(\mu\text{-}S)$ clusters interact with the alkyne, *e.g.* dpa to form a dithiolene $Mo_3(\mu_3\text{-}S)(\mu\text{-}S)(\mu_3\text{-}SC(Ph)=C(Ph)S)$ adduct under conditions of reversible equilibrium. The $[Mo_3S_4Cl_3(ImNH_2)]BF_4$ cluster salt is an efficient catalyst for the (*Z*)-selective semihydrogenation of dpa under much milder reaction conditions than those previously optimized for related diamino Mo_3S_4 cluster analogues. Mechanistic control experiments support a sulfur-based mechanism and rule out the operation of an outer sphere reaction mechanism with participation of the ligand NH group. Extension of our catalytic protocol to other internal alkynes revealed an excellent (*Z*)-selectivity. In addition, the catalytic protocol can also be adapted for the semihydrogenation of alkynols; in particular, to an essential vitamin E precursor. To the best of our knowledge, it is the first time that a homogenous molybdenum cluster performs this type of reaction.

Author contributions

The manuscript was written through contributions of all authors. All authors have given approval to the final version of the manuscript.

Conflicts of interest

There are no conflicts of interest to declare.

Acknowledgements

The financial support of the Spanish Ministerio de Economía y Competitividad (grants PRE2019-088511, and PID2019-107006GB-C22), Generalitat Valenciana (grant CIAICO/2021/122) and Universitat Jaume I (grants UJI-B2019-30, UJI-B2021-29 and UJI-B2022-56) is gratefully acknowledged. The authors also thank the Serveis Centrals d'Instrumentació Científica (SCIC) of the Universitat Jaume I for providing us with materials characterization facilities. Furthermore, we thank Leibniz-Institute for Catalysis for the facilities.

References

1 M. Crespo-Quesada, F. Cárdenas-Lizana, A. L. Dessimoz and L. Kiwi-Minsker, Modern trends in catalyst and process design for alkyne hydrogenations, *ACS Catal.*, 2012, **2**, 1773–1786.
2 B. Chen, U. Dingerdissen, J. G. E. Krauter, H. G. J. Lansink Rotgerink, K. Möbus, D. J. Ostgard, P. Panster, T. H. Riermeier, S. Seebald, T. Tacke and H. Trauthwein, New developments in hydrogenation catalysis particularly in synthesis of fine and intermediate chemicals, *Appl. Catal., A*, 2005, **280**, 17–46.
3 H. Lindlar, Ein neuer Katalysator für selektive Hydrierungen, *Helv. Chim. Acta*, 1952, **35**, 446–450.
4 D. Decker, H. J. Drexler, D. Heller and T. Beweries, Homogeneous catalytic transfer semihydrogenation of alkynes-an overview of hydrogen sources, catalysts and reaction mechanisms, *Catal. Sci. Technol.*, 2020, **10**, 6449–6463.
5 M. Garbe, S. Budweg, V. Papa, Z. Wei, H. Hornke, S. Bachmann, M. Scalone, A. Spannenberg, H. Jiao, K. Junge and M. Beller, Chemoselective semihydrogenation of alkynes catalyzed by manganese(I)-PNP pincer complexes, *Catal. Sci. Technol.*, 2020, **10**, 3994–4001.
6 V. Zubar, J. Sklyaruk, A. Brzozowska and M. Rueping, Chemoselective Hydrogenation of Alkynes to (Z) -Alkenes Using an Air-Stable Base Metal Catalyst, *Org. Lett.*, 2020, **22**, 5423–5428.
7 N. Gorgas, J. Brünig, B. Stöger, S. Vanicek, M. Tilset, L. F. Veiros and K. Kirchner, Efficient Z-Selective Semihydrogenation of Internal Alkynes Catalyzed by Cationic Iron(II) Hydride Complexes, *J. Am. Chem. Soc.*, 2019, **141**, 17452–17458.
8 C. Chen, Y. Huang, Z. Zhang, X. Q. Dong and X. Zhang, Cobalt-catalyzed (Z)-selective semihydrogenation of alkynes with molecular hydrogen, *Chem. Commun.*, 2017, **53**, 4612–4615.
9 H. Alawisi, H. D. Arman and Z. J. Tonzetich, Catalytic Hydrogenation of Alkenes and Alkynes by a Cobalt Pincer Complex: Evidence of Roles for Both Co(I) and Co(II), *Organometallics*, 2021, **40**, 1062–1070.
10 K. Semba, R. Kameyama and Y. Nakao, Copper-Catalyzed Semihydrogenation of Alkynes to Z-Alkenes, *Synlett*, 2015, **26**, 318–322.
11 Y. Liang, U. K. Das, J. Luo, Y. Diskin-Posner, L. Avram and D. Milstein, Magnesium Pincer Complexes and Their Applications in Catalytic Semihydrogenation of Alkynes and Hydrogenation of Alkenes: Evidence for Metal–Ligand Cooperation, *J. Am. Chem. Soc.*, 2022, **144**, 19115–19126.

12 N. F. Both, A. Spannenberg, K. Junge and M. Beller, Low-Valent Molybdenum PNP Pincer Complexes as Catalysts for the Semihydrogenation of Alkynes, *Organometallics*, 2022, **41**, 1797–1805.
13 A. G. Algarra, E. Guillamón, J. Andrés, M. J. Fernández-Trujillo, E. Pedrajas, J. Á. Pino-Chamorro, R. Llusar and M. G. Basallote, Cuboidal Mo_3S_4 Clusters as a Platform for Exploring Catalysis: A Three-Center Sulfur Mechanism for Alkyne Semihydrogenation, *ACS Catal.*, 2018, **8**, 7346–7350.
14 M. V. Joannou, M. J. Bezdek and P. J. Chirik, Pyridine (diimine) Molybdenum-Catalyzed Hydrogenation of Arenes and Hindered Olefins: Insights into Precatalyst Activation and Deactivation Pathways, *ACS Catal.*, 2018, **8**, 5276–5285.
15 T. Vielhaber, K. Faust and C. Topf, Group 6 Metal Carbonyl Complexes Supported by a Bidentate PN Ligand: Syntheses, Characterization, and Catalytic Hydrogenation Activity, *Organometallics*, 2020, **39**, 4535–4543.
16 E. Pedrajas, I. Sorribes, A. L. Gushchin, Y. A. Laricheva, K. Junge, M. Beller and R. Llusar, Chemoselective Hydrogenation of Nitroarenes Catalyzed by Molybdenum Sulphide Clusters, *ChemCatChem*, 2017, **9**, 1128–1134.
17 J. R. Cabrero-Antonino, E. Alberico, H.-J. Drexler, W. Baumann, K. Junge, H. Junge and M. Beller, Efficient Base-Free Hydrogenation of Amides to Alcohols and Amines Catalyzed by Well-Defined Pincer Imidazolyl–Ruthenium Complexes, *ACS Catal.*, 2016, **6**, 47–54.
18 R. Adam, E. Alberico, W. Baumann, H. J. Drexler, R. Jackstell, H. Junge and M. Beller, NNP-Type Pincer Imidazolylphosphine Ruthenium Complexes: Efficient Base-Free Hydrogenation of Aromatic and Aliphatic Nitriles under Mild Conditions, *Chem. – Eur. J.*, 2016, **22**, 4991–5002.
19 V. Papa, J. R. Cabrero-Antonino, E. Alberico, A. Spanneberg, K. Junge, H. Junge and M. Beller, Efficient and selective hydrogenation of amides to alcohols and amines using a well-defined manganese–PNN pincer complex, *Chem. Sci.*, 2017, **8**, 3576–3585.
20 *MassLynx, 4.1*, Waters Corporation, Milford, MA, 2005.
21 V. P. Fedin, M. N. Sokolov, Y. V. Mironov, B. A. Kolesov, S. V. Tkachev and V. Y. Fedorov, Triangular thiocomplexes of molybdenum: reactions with halogens, hydrohalogen acids and phosphines, *Inorg. Chim. Acta*, 1990, **167**, 39–45.
22 *CrysAlis, version 171.36.24*, Agilent Technologies, Santa Clara, CA, 2012.
23 R. C. Clark and J. S. Reid, *Acta Crystallogr., Sect. A: Found. Crystallogr.*, 1995, **51**, 887–897.
24 G. M. Sheldrick, *Acta Crystallogr., Sect. A: Found. Crystallogr.*, 2008, **64**, 112–122.
25 O. V. Dolomanov, L. J. Bourhis, R. J. Gildea, J. A. K. Howard and H. Puschmann, *J. Appl. Crystallogr.*, 2009, **42**, 339–341.
26 K. Brandenburg and H. Putz, *DIAMOND, Crystal Impact GbR*, Bonn, Germany, 2005.
27 E. Pedrajas, I. Sorribes, K. Junge, M. Beller and R. Llusar, A Mild and Chemoselective Reduction of Nitro and Azo Compounds Catalyzed by a Well-Defined Mo_3S_4 Cluster Bearing Diamine Ligands, *ChemCatChem*, 2015, **7**, 2675–2681.
28 T. F. Beltrán, J. Á. Pino-Chamorro, M. J. Fernández-Trujillo, V. S. Safont, M. G. Basallote and R. Llusar, Synthesis and structure of trinuclear W_3S_4 Clusters bearing aminophosphine ligands and their reactivity toward halides and pseudohalides, *Inorg. Chem.*, 2015, **54**, 607–618.
29 A. L. Gushchin, Y. A. Laricheva, P. A. Abramov, A. V. Virovets, C. Vicent, M. N. Sokolov and R. Llusar, Homoleptic Molybdenum Cluster Sulfides Functionalized with Noninnocent Diimine Ligands: Synthesis, Structure, and Redox Behavior, *Eur. J. Inorg. Chem.*, 2014, 4093–4100.
30 J. A. Pino-Chamorro, Y. A. Laricheva, E. Guillamón, M. J. Fernández-Trujillo, E. Bustelo, A. L. Gushchin, N. Y. Shmelev, P. A. Abramov, M. N. Sokolov, R. Llusar, M. G. Basallote and A. G. Algarra, Cycloaddition of alkynes to diimino Mo_3S_4 cubane-type clusters: a combined experimental and theoretical approach, *New J. Chem.*, 2016, **40**, 7872–7880.
31 A. G. Algarra and M. G. Basallote, in *Advances in Inorganic Chemistry*, ed. C. D. Hubbard and R. van Eldik, Academic Press, 2017, vol. 8, pp. 311–342.
32 Y. Ide, M. Sasaki, M. Maeyama and T. Shibahara, Adducts of Acetylene and Dimethylacetylenedicarboxylate at Sulfurs in Sulfur-Bridged Incomplete Cubane-Type Tungsten Clusters, *Inorg. Chem.*, 2004, **43**, 602–612.
33 E. Guillamón, M. Oliva, J. Andrés, R. Llusar, E. Pedrajas, V. S. Safont, A. G. Algarra and M. G. Basallote, Catalytic Hydrogenation of Azobenzene in the Presence of a Cuboidal Mo_3S_4 Cluster via an Uncommon Sulfur-Based H_2 Activation Mechanism, *ACS Catal.*, 2021, **11**, 608–614.
34 R. Kusy, M. Lindner, J. Wagner and K. Grela, Ligand-to-metal ratio controls stereoselectivity: Highly functional-group-tolerant, iridium-based, (E)-selective alkyne transfer semihydrogenation, *Chem. Catal.*, 2022, **2**, 1346–1361.
35 K. Baldenius, L. von dem Bussche-Hünnefeld, E. Hilgemann, P. Hoppe and R. Stürmer, in *Ullmann's Encyclopedia of Industrial Chemistry*, Wiley-VCH Verlag GmbH & Co. KGaA, Weinheim, Germany, 2021, pp. 1–21.

